



CAN UNCLASSIFIED



DRDC | RDDC
technologysciencetechnologie

Sensitivity of polymer-bonded explosives from molecular modeling data

David Brochu
CERMA and CQMF, Université Laval

Hakima Abou-Rachid
DRDC – Valcartier Research Centre

Armand Soldera
Centre Québécois sur les Matériaux Fonctionnels, Faulté des sciences, Université de Sherbrooke

Josée Brisson
CERMA and CQMF, Université Laval

International Journal of Energetic Materials and Chemical Propulsion
DOI: 10.1615/IntJEnergeticMaterialsChemProp.2018021264

Date of Publication from Ext Publisher: July 2018

Defence Research and Development Canada

External Literature (P)

DRDC-RDDC-2018-P091

July 2018

CAN UNCLASSIFIED

CAN UNCLASSIFIED

IMPORTANT INFORMATIVE STATEMENTS

This document was reviewed for Controlled Goods by Defence Research and Development Canada (DRDC) using the Schedule to the *Defence Production Act*.

Disclaimer: This document is not published by the Editorial Office of Defence Research and Development Canada, an agency of the Department of National Defence of Canada but is to be catalogued in the Canadian Defence Information System (CANDIS), the national repository for Defence S&T documents. Her Majesty the Queen in Right of Canada (Department of National Defence) makes no representations or warranties, expressed or implied, of any kind whatsoever, and assumes no liability for the accuracy, reliability, completeness, currency or usefulness of any information, product, process or material included in this document. Nothing in this document should be interpreted as an endorsement for the specific use of any tool, technique or process examined in it. Any reliance on, or use of, any information, product, process or material included in this document is at the sole risk of the person so using it or relying on it. Canada does not assume any liability in respect of any damages or losses arising out of or in connection with the use of, or reliance on, any information, product, process or material included in this document.

© Her Majesty the Queen in Right of Canada (Department of National Defence), 2018

© Sa Majesté la Reine en droit du Canada (Ministère de la Défense nationale), 2018

CAN UNCLASSIFIED

Sensitivity of Polymer-Bonded Explosives from Molecular Modeling Data

David Brochu^{1,2}, Hakima Abou-Rachid¹, Armand Soldera³ & Josée Brisson²

¹ Defence Research & Development Canada – Valcartier Research Centre, Government of Canada 2459 de la Bravoure Road, Québec, QC, Canada, G3J 1X5

² Département de chimie, CERMA (Centre de recherche sur les matériaux avancés) and CQMF (Centre Québécois sur les Matériaux Fonctionnels), Faculté des sciences et de génie, Université Laval, Québec, Canada G1V 0A6

³ Département de chimie, Centre Québécois sur les Matériaux Fonctionnels, Faculté des sciences, Université de Sherbrooke, Québec, Canada J1K 2R1

© Her Majesty the Queen in Right of Canada, as represented by the Minister of National Defence, [2017]

Key Words: PBX, Energetic materials, Molecular modeling, RDX, HTPB, Computational chemistry

Abstract

Sensitive energetic materials are an issue for military and civilian applications. To prevent undesired explosions, sensitive energetic materials are embedded in a protective polymer, resulting in polymer-bonded explosives (PBX). The appropriate polymer will absorb part of the energy caused by stimuli such as shock, impact, friction and heat, thus decreasing sensitivity. To investigate how an appropriate polymer absorbs energy, three PBX models were simulated using molecular dynamics. The COMPASS force field implemented in the Materials Studio software

was used. Molecular dynamics simulations were performed for three RDX-based formulations in which a single polymer chain (HTPB, ESTANE or EVA) was placed at the boundary surface of an RDX crystal. Simulations were carried out at high temperature (700K) and high pressure (15GPa). Resulting models were analyzed in terms of potential energy increase, energy distribution and values of the different potential energy contributions for RDX/HTPB, RDX/Estane and RDX/EVA. The polymer binders HTPB, Estane and EVA in such PBX formulations absorbed between 24 and 31% of internal energy respectively, thereby making less sensitive PBXs formulations than pure RDX. This percentage is proposed as an indicator key for experimentalists to determine the most efficient polymer that can be used, for a given explosive, to minimize munition sensitivity. A clear correlation is established between the calculated absorption of internal energy by polymers and experimental sensitivity values for the three formulations studied under extreme experimental conditions. This approach may be applied to other new formulations prior to testing them in laboratories.

1. Introduction

Over the last three decades, there has been an increase in undesirable detonations of explosives across the world (Small Arm Survey, 2012) and these have severe consequences in terms of loss of lives and equipment. These detonations have been mostly related to the transportation, storage and handling of excessive quantities of explosives. This has led to significant research effort to develop explosives that are less sensitive to stimuli. Sensitivity is defined as the ease with which an explosive can set off (Agrawal, 2010). Many types of stimuli can initiate an explosive detonation, for instance shock, impact, heat, friction and electrostatic discharges (Field, 1992). Explosives molecules are often crystalline substances that can be embedded in a protective polymer coating whose role is to absorb the energy of a shock wave resulting from a stimulus. Blends of explosives and polymers, designated as polymer-bonded explosives (PBXs), are used in various applications such as demolition explosives or warhead high explosives (Daniel, 2006). If the energy or a part of it does not reach the energetic crystals, initiation does not occur, significantly reducing the sensitivity of the explosive.

Research on reduced sensitivity explosive formulations is a slow and expensive process, due to explosion hazards. Understanding and predicting explosives sensitivity has therefore drawn the attention of many research groups (Abou-Rachid et al., 2008; Jaidann et al., 2008; Li et al., 2011a,b; Politzer and Murray, 2003; Qiu et al., 2007; Xiao et al., 2008; Xu et al., 2006, 2007; Zhu et al., 2009). Molecular modeling and simulations of explosives provide a useful approach to understanding the problem (Mathieu, 2013; Mathieu and Alaime, 2014). Although these methods cannot quantitatively predict the sensitivity of explosives, correlations could be established between experimental sensitivity measurements and parameters estimated from

simulations. These correlations have already shown to offer some physical insights regarding the sensitivity of explosive crystals (Belik et al., 1999, Chaoyang et al., 2005, Jun et al., 2006, Kamlet and Adolph, 1979, Rice and Hare, 2002). In most of the reported work, only the explosives crystals were studied, whereas most current explosives, such as PBXs, are complex, multiphase mixtures (Agrawal, 2010). The interface between the energetic crystals and the protective polymer/plasticizer, to which various additives can also be added, have been the object of only a few computational studies using the molecular mechanics approach. (Abou-Rachid et al., 2008; Brochu et al., 2013; Jaidann et al., 2008, 2009; Li et al., 2011, Qiu et al., 2007; Xiao et al., 2008; Xu et al., 2006, 2007; Zhu et al., 2009) Molecular modeling has not been used as yet to investigate the sensitivity of PBX. Because of the lack of predictive methods for sensitivity, most research in polymer-bonded explosives is still mostly based on long, expensive and hazardous testing methods. Developing a modeling tool to predict sensitivity of complex formulation such as PBX would limit expensive and dangerous experimental work by pre-screening possible material candidates thereby limiting the number of test required in the development of insensitive energetic materials.

There is consensus in the energetic materials community that detonation of an explosive starts within an area of high thermal energy called hotspot (Czerski and Proud, 2007). An energy stimulus must be converted into heat for a hotspot to occur (Bowden and Yoffe, 1952). To start a detonation, the specific area that will become a hotspot must last between 0.1 to 10 μm and the energy must be concentrated in an area between 10 μs to 1 ms. The temperature must be maintained at around 700 K. The hotspot formation probability depends on many factors such as the type of explosive, the size of the energetic crystals (when the energetic molecule is crystalline) and the nature of the polymer matrix covering the explosive. Many mechanisms have

been proposed and described in the literature regarding a hotspot formation, and are still the object of much debated discussions. Proposed mechanisms include adiabatic compression of gases by rapid collapse of gas bubbles (Chaudhri and Field, 1974; Coley and Field, 1973), friction between crystals, internal surface or extraneous grit particles (Bowden and Yoffe, 1952; Rideal and Robertson, 1948), shear band formation (Afanas'ev and Bobolev, 1970), heating of crack tips or dislocation pileups (Coffey, 1981), along with many others (Field, 1992, Field et al., 1982).

Most mechanisms explaining hotspot formation involve changes at the microscopic and molecular scale. Molecular dynamics (MD) simulations can be a useful tool to capture effects at this scale. In this work, an approach based on analysis of how energy is distributed in the explosive following specific stimuli is proposed. The goal is to understand how the polymers affect the energy distribution at the molecular level. Changes are occurring at very short times in the plastic regime, before the energy reaches the explosive crystal. Understanding how the energy is distributed in the polymer in the vicinity of an explosive crystal could lead to determining sensitivity of specific formulations.

The determination of the sensitivity of most common explosive crystals experimentally is very well documented and could be used to validate the appropriateness of the models. In this work, model systems were chosen with respect to data availability. Three different models of the interface between an amorphous polymer, with or without plasticizers depending on available experimental data, were chosen. In all cases, the explosive crystal was 1,3,5-trinitro-1,3,5-triazinane (RDX), given that it is the most common energetic molecule used in explosives. The three models consisted of a different amorphous polymeric phases, hydroxy-terminated polybutadiene (HTPB) plus dioctyladipate (DOA) plasticizer, Estane® and ethyl vinyl acetate

(EVA). These were considered based on their military use, their chemical composition, the fact that they had different chemical structures and the availability of experimental data. Simulations were carried out on models at temperatures and pressures corresponding to reasonable experimental hotspot formation conditions. The different potential energy contributions were analyzed to reveal energetic changes induced by these stimuli at short timescales, leading to a better understanding of the behavior of PBXs.

2. Methodology

The simulations were performed using the Materials Studio (MS) 4.3 software (2008). The force field used throughout this work was COMPASS (Condensed-Phase Optimized Molecular Potentials for Atomistic Simulation Studies) (Sun, 1998). COMPASS is a class II *ab initio* force field conceived to represent the interactions in condensed materials. In the optimization of this force field, specific attention was given to the energetic materials, functional nitro (Yang et al., 2000) and nitrate esters groups (Bunte and Sun, 2000). The COMPASS force field is therefore well parameterized and suitable for the formulations studied in this work.

Minimizations were carried out using the Smart Minimizer approach of Materials Studio. This approach consists of three successive minimization steps that use steepest descent, conjugate gradients and a Quasi-Newton Broyden-Fletcher-Goldfarb-Shanno (BFGS) minimization. Non-bonded interactions calculations were truncated at 0.95 nm using a spline width of 0.1nm and buffer width of 0.05 nm. Periodic boundary conditions were imposed.

MD simulations were carried out using two different ensembles depending on the chosen stimuli. NVT (constant number of atoms, volume and temperature) and NPT (constant number of atoms, pressure and temperature) ensembles were used. The temperature and pressure were controlled

using the Andersen method (Andersen, 1980). The velocity-Verlet method was used to integrate the Newton equation with an integration time step of 1 fs.

To build a cell representative of the most common PBX formulations, the technique used was the same that was defined by our group (Brochu et al., 2013). PBX formulations were built by superimposing a crystalline RDX layer onto an amorphous cell containing the polymeric chain and the plasticizer, when used. The resulting cell was then submitted to a series of compression/minimization steps small enough to keep the crystal cell structure, as verified by radial distribution function calculations. The compression/minimization simulations were run until a minimum energy cell was obtained. Two cells of each of the three formulations were built in order to insure simulation reliability. Results presented throughout this article are the average of these two cells unless otherwise stated. The resulting cells were used as a starting point to carry out simulations at high temperature and high pressure.

The crystalline RDX layer was built using atomic positions and cell dimensions of the crystal structure experimentally determined by Choi and Prince (1972). RDX crystallizes in the orthorhombic space group *Pbca* with $a = 13.182 \text{ \AA}$, $b = 11.574 \text{ \AA}$ and $c = 10.709 \text{ \AA}$. The unit cell contained eight RDX molecules. The crystalline layer was defined as a combination of 18 unit cells combined in a single $3 \times 2 \times 3$ array cleaved at the (2 0 0) plane. The (2 0 0) plane was chosen because it is most commonly observed at the surface of the solution-crystallized RDX crystals (van der Heijden and Bouma, 2004).

The amorphous phase was built using a single polymeric chain under periodic boundary conditions, instead of numerous small molecules, in order to investigate configuration changes of the chain when submitted to stress. The use of a single chain is proposed to better represent

realistic explosives, as plastic chains are normally cross-linked with PBXs. This chain was inserted in a large cell under periodic boundary conditions to simulate an infinite layer of amorphous material. For HTPB, this chain was 80 repeated units long, with a molar mass of 4 354 Da, with proportions of 60% *trans*, 20% *cis* and 20 % vinyl butadiene groups with hydroxyl end-groups. Eight molecules of the DOA plasticizer were added to the HTPB models to reproduce the experimental formulation of this specific PBX. The Estane chain is composed of six groups each one composed of five successive ester monomers and one urethane monomer (5/1 proportion), with one hydrogen and one methyl end-group, for a total molecular weight of 8,056 Da. The EVA chain was composed of 160 ethyl repeat units and 40 vinyl acetate repeat units (80/20 proportion) with two hydrogen end-groups, for a total molecular weight of 7,920 Daltons. All polymers were generated using the Amorphous_Cell code which is part of the Materials Studio package and are based on the modified self-avoiding walk procedure stemming from the Theodorou-Suter and Meirovitch methods (Meirovitch, 1983; Theodorou and Suter, 1986). Despite the fact that this procedure does not take into account the entropy effect (Matheson, 1987), reaching the mechanical equilibrium helps to overcome this issue (Metatla and Soldera, 2011). The target density was fixed to 0.90 g/cm^{-3} at 298K, which is the experimental density of military-grade HTPB (Sartomer Company, 2011). Cell parameters a and b were fixed to fit with the size of the crystalline layer.

To build the final PBX models, the amorphous cells selected for each polymer (HTPB-DOA, Estane or EVA) were superimposed to the previously constructed crystalline layer using the Materials Studios Layer Building Tool. The unit cell is elongated along the z axis (unit c parameter) to allow it to house the full polymer chain (this corresponded to approximately

doubling the c parameter). The crystalline cell is then placed on top of the amorphous cell, and the c parameter of the resulting supercell is taken as the sum of the two superimposed unit cells.

Segmental loops extend away from the polymer layer when the chain is isolated, as is shown in Fig. 2. This operation results in the inclusion of empty spaces. When the crystalline and amorphous layers are joined, the resulting supercell is not at the correct experimental density and a series of compression/minimization steps was performed, as shown in Fig. 3, to provide a more realistic formulation with a density that corresponds to the mechanical equilibrium (Zhu et al., 2009). Figure 3 shows the potential energy of each PBX supercell simulated at each step of the minimization/compression protocol. With this procedure, a density equalled to the experimental density was reached without affecting the crystalline phase. The compression/minimization procedure was carried out until an increase in the potential energy of the whole formulation was observed. A refinement step with changes of 0.01 \AA was then carried out to reach a minimum in energy with respect to cell volume. The mechanical equilibrium is therefore reached at the bottom of each energy well (Zhu et al., 2009).

To simulate conditions prior to detonation, PBX cells were submitted to two different stimuli: A high temperature of 700 K, and a high pressure of 15 GPa. The selected temperature of 700K corresponds to the typical temperature of hotspots (Bowden and Yoffe, 1952). The chosen high pressure of 15 GPa is arbitrary since no specific pressure related to hotspots formation for PBXs was found in the literature. However, during detonation, an increase in pressure leads to an increase in thermal energy. This conversion is influenced by large number of factors such as density, void, explosive crystal size and crystalline plane surfaces. The value of 15 GPa was chosen as it is sufficiently high to take into account these effects.

The supercells thus built and minimized were used to carry out the MD simulations. A first simulation in the NVT ensemble was performed at room temperature for 250 ps to obtain a cell without any induced stress. Simulations were then carried out in the NVT ensemble at room temperature (RT) or 298K and at the higher temperature of 700K. In parallel, simulations in the NPT ensemble were carried out at 0 GPa, to simulate ambient condition, and at 15 GPa to simulate high pressure stimuli. The series of MD simulations under NPT conditions at 0 GPa were used to estimate mechanical properties. For this specific pressure, the Parrinello barostat (Parrinello and Rahman, 1982) was more appropriate. In all cases, simulations were carried out for 250 ps and a frame was saved at each picosecond.

3. Results and discussion

As a first analysis, total potential energy of formulations were compared before and after the stimulus were applied, to identify the formulation with the highest energy under the given temperature or pressure conditions. Therefore, the high temperature dynamics simulations carried out in the NVT ensemble were compared to the room temperature NVT MD simulations. Likewise, the high pressure dynamics simulations performed in the NPT ensemble were compared to the 0 GPa NPT MD. The observed increase in the energy and the percentage the energy change are shown in Table 1. Each value reported in Table 1 corresponds to an average over the last ten frames of each MD trajectory. This was further averaged over the two different, low-energy supercells used. Errors were estimated as standard deviations.

Table 1 – Energy increase (kcal/mol and %) for the PBX models simulated at 700K and 15GPa

	Method	Energy		Energy difference	
		E_{initial}	E_{final}	(kcal.mol ⁻¹)	(%)

		(kcal.mol ⁻¹)	(kcal.mol ⁻¹)		
RDX/HTPB	NVT, 700K	-26198±7	-20229±7	5970±5	30
RDX/ESTANE		-27020±10	-21350±20	5670±30	27
RDX/EVA		-27450±30	-21420±10	6030±10	28
RDX/HTPB	NPT, 15GPa, 298K	-26025±7	-18710±40	7320±50	39
RDX/ESTANE		-26910±20	-19628±8	7280±7	37
RDX/EVA		-27340±20	-19700±70	7640±50	39

As shown in Table 1, the increase in potential energy is systematically higher for NPT than for NVT conditions. The 15 GPa pressure increase cannot be explicitly correlated to the 700 K temperature increase. There are unfortunately no data available in the literature for which the relative contributions of temperature and pressure to hotspot formation can be compared (Bowden and Yoffe, 1952; Field et al., 1982). The 15 GPa value was selected by trial and error to give final energy values in the same range as that of the 700K dynamic simulations, but the fit between the two was not totally optimized and the two condition sets are not necessarily energetically or phenomenologically equivalent. For example, for RDX/EVA formulations submitted to a temperature stimulus, the energy increases to 5,670 kcal/mol for RDX/ESTANE and to 6,030 kcal/mol for RDX/EVA, which represents an energy increase of 27 and 30%, respectively. These values are slightly higher in the case of a high pressure stimulus, with an energy increase of 7,280 kcal/mol for RDX/ESTANE and 7,640 kcal/mol for RDX/EVA (37 and 39 %, respectively).

The formulation with the highest increase in energy at 700K is RDX/EVA, followed by RDX/HTPB and RDX/Estane. Similar trends are found for simulations under 15 GPa pressure. These results reveal that each formulation behaves differently when submitted to the same stimulus.

It is important to note that, during the timeframe in which the simulations are conducted, the energy increase is reversible: if the formulation is returned to ambient conditions, the energy is restored to its original value, prior to applying a high temperature or a high pressure stimulus. This has been verified using calculations on RDX/HTPB. For this formulation, using the model obtained after a 700K NVT molecular dynamics simulation, a second simulation was carried out at 298K NVT for 250 ps, and the resulting energy returned, within experimental error, to its original value, a decrease in energy of 0.6% being obtained as compared to the original energy of -26,191 kcal/mol. The same calculation was performed for the high pressure stimulus and the result is a 0.4% decrease in energy which is well within expected statistical fluctuations for this method. Not only does the formulation return to being energetically equivalent to its original conformation after relaxation but the crystalline part of the supercell is not significantly altered by the stimulus. These observations are related to the limited simulation time used, which does not allow for long-range rearrangements and conformation changes and cause deformations to remain in the elastic regime.

Knowing that the increase in the potential energy of each formulation is different, even under the same conditions, as shown in Table 1, it is worthwhile to understand how this energy increase distributes within the formulation. The potential energy increase was thus calculated separately for each of the two formulation phases: the amorphous polymeric chain phase (including the plasticizer) and the crystalline explosive phase as shown in Fig. 4. The potential energies are

shown in Fig. 5. The values shown correspond to the average increase in energy of the polymer and the explosive for the two supercells of each PBX formulation.

In Table 2, for each formulation, the crystalline phase always exhibits the highest energy increase. This is not surprising given the explosive/polymer ratio of each formulation. More interesting is that in all cases, increases in the energy of the explosive sub-cell of each formulation are very similar from one formulation to another for a given stimulus. The standard deviation for the energy increase of the explosive is only 1% for the high temperature stimuli, and 2% for the high pressure stimuli. This indicates that, for a given stimulus, the explosive crystal reacts independently from the polymeric chain surrounding it.

The polymeric sub-cell reacts differently. The polymer increase in energy is different for each formulation, for a given stimulus, with standard deviations ranging from 8 to 11 %. This clearly indicates that energy changes are mostly concentrated in the polymer and vary from one polymer to another. The choice of the polymer will therefore have the largest effect on the sensitivity as expected.

It has been known that the polymer is not only the first protection barrier, but that it has also the potential to absorb and store energy. To estimate the energy storage, energy increase percentage was calculated for each of the two phases, crystalline and amorphous. The energy increase percentage was calculated for each component by dividing the energy of a specific phase (or sub-cell) by that of the whole formulation (or supercell). The values correspond to those of the polymer sub-cell and are shown in Table 2.

Table 2 - Percentage of energy stored by the polymer of the PBX formulation during 700K and 15GPa simulations

	RDX/HTPB	RDX/ESTANE	RDX/EVA
NVT, 700K	30%	26%	31%
NPT, 15GPa, 298K	26%	24%	28%

As already shown, the crystalline explosive phase absorbs more energy than the polymer phase given that the explosive accounts for 80 weight % of the formulation. However, the energy increase observed for the polymer phase alone, varying from 24 to 31%, is higher than the 20 weight percent difference. This is in agreement with the intrinsic nature of the polymer, which is more flexible and is capable to absorb more energy by adopting high-energy conformations. This energy is trapped, and is not available to form hotspots thus decreasing the risk of detonation.

When each formulation is analyzed individually, RDX/EVA exhibits the highest energy storage of both stimuli conditions simulated and this account for 28 and 31 % of the energy provided to the formulation. RDX/HTPB energy storage is similar with values ranging from 26 to 30%. RDX/Estane shows the worst storage performance with only 24 to 26% energy absorbed. Thus, it is predicted on this basis that RDX/EVA should show the lowest sensitivity.

An assessment was also performed to determine which potential energy term was the most affected under each stimuli condition. Potential energy can be divided into two main contributions, non-bond energy (van der Waals, Coulombic or electrostatic and H-bond energy) and the internal energy (bond and angle deformation, torsion and cross-terms) (Soldara, 2002). In the COMPASS forcefield, the H-bond energy cannot be separated from the van der Waals (vdW) term and will therefore not be discussed here. Internal energy is further separated into the valence energy and energy cross-terms and the valence energy being of the energy related to

bond distance deformation, bond angle deformation, torsions, changes in out-of-plane contributions and 1-3 Urey-Bradley energy, which is negligible in this case.

$$E_{potential} = E_{Internal} + E_{non-bond} \quad (1)$$

$$E_{non-bond} = E_{vdW} + E_{Coulomb} + E_{H-bond} \quad (2)$$

$$E_{Internal} = E_{valence} + E_{crossterm} \quad (3)$$

$$E_{Valence} = E_{bond} + E_{angle} + E_{torsion} + E_{oop} + E_{UB} \quad (4)$$

Percentage increase for given components as compared to that of the whole polymer sub-cell are given in Table 3 for the three polymers. The values correspond to the average of the two supercells simulated in each case.

Table 3 – Energy increase (kcal/mol) and percentage of energy absorbed by the complete formulation, explosive and polymer, per component, at 700K and 15GPa

	Method	Energy	ΔE_{comp} (kcal.mol ⁻¹) 1)	ΔE_{exp} (kcal.mol ⁻¹) 1)	ΔE_{poly} (kcal.mol ⁻¹) 1)	ΔE_{poly} (%)
RDX/HTPB	NVT 700K	Total	5970	4196	1771	30
		-Internal	4733	3167	1546	33
		-Non-	1236	1028	224	18

		bond				
	NPT 15GPa	Total	7320	4942	1867	26
		-Internal	1559	1150	409	26
		-Non-bond	5761	3792	1458	25
RDX/ESTANE	NVT 700K	Total	5665	4171	1476	26
		-Internal	4502	3207	1295	29
		-Non-bond	1164	964	181	16
	NPT 15GPa	Total	7282	5135	1724	24
		-Internal	1527	1173	353	23
		-Non-bond	5756	3962	1371	24
RDX/EVA	NVT 700K	Total	6028	4146	1887	31
		-Internal	4816	3169	1647	34
		-Non-bond	1211	977	239	20
	NPT 15GPa	Total	7637	5057	2157	28
		-Internal	1799	1139	661	36
		-Non-bond	5838	3918	1497	26

The first observation that stands out from Table 3 is the difference between internal energy and non-bond energy changes when compared to the 700K NVT and the 15 GPa NPT simulations. Internal energy increases are higher for the NVT simulations, whereas, in the NPT simulations,

the van der Waals energy increase is higher. Both internal and non-bond energies increase during simulations, but to different extents. As the temperature increase, Brownian motions in the polymeric chain and in the plasticizer molecules are increased. Part of the thermal energy is stored through increases in bond lengths and angles. This contributes to increasing the internal energy of the polymeric phase in the NVT simulations. The difference observed in the increase in energy of the NPT ensemble, which is the heat capacity at constant pressure, stems from the fact that additional PV work is added to the formulation. In this case, this higher amount of energy is reflected mainly in the non-bond energy terms.

As the pressure increases, repulsive Coulombic interactions increase and dispersive Coulombic interactions decrease, resulting in a net increase in the non-bond energy and this leads to destabilization of the formulation. This can be related to the observed decrease in unit cell dimensions, which forces the atoms closer to one another, contrary to what occurs in NVT dynamics. NPT simulations allow cell parameters to change, and under a 15 GPa pressure value, an average density compression of 0.5 g/cm^3 is observed which corresponds to a 33% increase. Under these conditions, as shown in the simulations, cell parameters return to their original values when the pressure stimulus is removed as deformation remains in the elastic regime. From a qualitative standpoint, as shown in Table 3, the most important changes in energy are observed for the internal energy. This is in agreement with the assumption that the polymer chain mainly absorbs energy by changing its internal conformation under these conditions.

Figure 6 shows the contributions of each internal energy parameters in the polymer. As discussed earlier, RDX/EVA exhibits the highest increase in energy. For the three most prominent internal energy terms in the NVT simulations, bond deformation, angle deformation and torsion, RDX/EVA exhibits the most significant increase, followed by RDX/HTPB and RDX/Estane. The highest increase observed is in the angle deformation energy, with RDX/EVA showing the highest increase percentages. Bond deformation follows. The fact that the torsional energy is the least important term indicates that there is no significant rearrangement of the chain in the timeframe studied.

In the NPT simulations, RDX/EVA also shows the highest increase in energy, but 75.4% of this increase is due to torsion angle deformation. A correlation shows that the most prominent energy terms (bond deformation energy for NVT simulations and torsional energy for NPT simulations) will point to the formulation that would be the least sensitive. For this simulation, bond and angle deformation terms are higher in RDX/HTPB and RDX/EVA, showing that chain flexibility plays a role in the observed energy distribution.

Knowing that deformation and torsion of the chain account for a large proportion of the energy increase, it becomes worthwhile to predict and compared mechanical properties of these systems. These were estimated from separate simulations using the Theodorou approach (Theodorou and Suter, 1986) using the NPT simulations at 298K and 0 GPa. Table 4 reports the resulting estimated mechanical properties of the formulations for the most stable cell of each PBX.

Table 4 – Estimated mechanical properties of the formulations (in GPa) at 298K and 0GPa

	RDX/HTPB	RDX/ESTANE	RDX/EVA
Tensile Modulus (E)	2.696	2.716	1.940
Poisson's Ratio (ν)	0.3791	0.3991	0.4322
Bulk Modulus (K)	3.716	4.486	4.766
Shear Modulus (G)	0.9776	0.9706	0.6772

As shown in Table 4, RDX/EVA which is the formulation showing the highest energy absorption or storage, is also the one with the lowest tensile and shear moduli. This indicates that RDX/EVA is more ductile, and can be correlated to the ease of storing energy. RDX/EVA also displays the highest Poisson's Ratio, with an average value of 0.43, a value closer to the value expected for a rubber with a ratio of 0.5 rather than of a rigid polymer with a ratio of 0.3. These observations are also consistent with the initial assumption that changes in the chain conformation and polymer interactions are the main mechanisms for energy absorption in these formulations. RDX/HTPB and RDX/Estane are very similar, although RDX/Estane has a higher bulk modulus. Estane is known to be the toughest and most rigid polymer of the three, which agrees well with the previous energy absorption analysis. This may be related to the fact that simulations were performed on a unit cell comprising of an amorphous cell, a crystalline layer and includes an interface. The size of the unit cell is appropriate for mechanical property calculations, as shown by Soldera et al. (Soldera, 2012). In this specific case, it is suspected that the interface plays a major role, and as the size of the interface is very limited in these calculations, this could have led to large fluctuations observed. Further work is definitely needed to optimize such formulations for mechanical property calculations.

Estimations of PBX mechanical properties are subject to larger variations, and could not be correlated significantly to sensitivity theory and analysis. Mechanical property simulations are faster than the energy simulations done here, but the energy results may be more reliable. They show a good convergence, with each cell resulting in similar energies, and may provide better parameters to predict sensitivity of PBXs.

Validation is an extremely important step in simulation but for PBXs, very few experimental data has been published regarding sensitivity. As a result for this study, data for a common explosive formulation with equal explosive concentration were chosen with respect to existing data. Experimental data published by T. Nath and S.N Asthana (Joseph et al., 2009, Nath et al., 1997) of the High Energy Materials Research Laboratory in two different studies on RDX-based sheet explosive were therefore used. In their work, explosives were made using 5-6 μm particle size RDX with partially gelatinized polymers at 40-50 $^{\circ}\text{C}$. RDX/HTPB contained an unspecified amount of DOA (Joseph et al., 2009), but it is assumed that it is between 30 to 50%, similar to the other RDX/HTPB formulations reported. RDX/EVA and RDX/Estane contained 1 to 2 % DOA, which was not included in the model used in this study based on the small amount of each (Nath et al., 1997).

In these two articles, sensitivity has been estimated by two tests, which are the drop weight impact sensitivity test (H_{50}) and the gap test. The drop weight impact test was done using the fall hammer method with a 2 kg weight as per the Bruceton staircase approach (Dixon and Mood, 1948). The shock sensitivity was measured using the gap test. For RDX/Estane and RDX/EVA explosives, the aluminum block gap test was used, using 63 mm of diameter aluminum block (Yadav et al., 1994). RDX/HTPB tests were done using the more conventional small scale N.O.L card gap test using cellulose acetate sheets (Price and Liddiard, 1966). Pressure values are

calculated using the sheet thickness. The pressures reported in the literature are summarized in Table 5.

Table 5 – Sensitivity data for the three RDX-based PBX formulations as reported in the literature (Joseph et al., 2009, Nath et al., 1997).

Formulation	RDX/HTPB		RDX/ESTANE		RDX/EVA	
	85/15	80/20	85/15	80/20	85/15	80/20
Drop Weight Impact Sensitivity Test (H_{50}) Height (cm)	75	NA	73	82	80	85
GAP Test Pressure - GPa	18.0	NA	7.34	7.88	6.83	7.6

NA: not available

Experimental values are available for two RDX/Estane and RDX/EVA composition ratios, 80/20 and 85/15. Unfortunately, for RDX/HTPB, values have been published only for the 85/15 proportion (Nath et al., 1997). All these explosives were made with RDX particles or crystals of 5-6 μm size. A plasticizer, dioctyl phthalate (DOP), was included in a concentration of 1 to 2 % for these explosives.

As shown in Table 5, the two tests yield different results. RDX/EVA compositions exhibit the best performance for the drop weight impact test, followed by RDX/HTPB and RDX/Estane, whereas RDX/HTPB yields the best results in the GAP test. It must however be noted that, in the case of the RDX/HTPB study, RDX particles were coated with DOP, which further lowers the sensitivity.

However, notwithstanding for the drop weight impact test, the reported experimental sensitivity results show the similar trends as those stemming from molecular simulation, which is, RDX/EVA, a more ductile polymer, is the least sensitive, followed by RDX/HTPB and RDX/Estane. The same conclusion can be made that sensitivity is lowered by the polymer which absorbs part of the energy, thus decreasing or delaying hotspot formation in PBXs.

4. Conclusion

Molecular simulations of three PBX formulations provide useful information based on the energy partition on how the explosives respond to the stress and how the polymer coating could provide additional protection to the crystalline structure RDX. When a stress is applied, all explosives examined show similar increases in energy. Differences are mainly observed in the polymer phase. RDX/EVA shows the greatest energy absorption, followed by RDX/HTPB and RDX/Estane. Scaled to the weight fraction of each phase, the increase was higher for the polymer than for the explosive, which is in agreement with the known effects of the polymer on sensitivity of PBXs. The increase in energy was mainly concentrated in the bond deformation, angle deformation and angle torsion terms. Mechanical properties were estimated by MD simulations and showed that EVA is the most ductile polymer which is in agreement with the conclusions that deformation of this polymer leads to the highest energy absorption in MD

simulations. These results are also in agreement with the relative sensitivity order of these formulations, as estimated from experimental drop weight impact test results reported in the literature. These results highlight the predictive capabilities of all-atom molecular simulation, within their intrinsic limits, as these methods do not allow exploring deformations induced in the plastic regime. It is proposed that molecular modeling simulations could be a useful tool to screen possible candidates and select the less sensitive formulations. This pre-screening decreases the number of systems to be experimentally prepared and tested, and thus decreases time and cost of energetic materials development.

5. Acknowledgments

The authors wish to acknowledge the support of Calcul Québec and the Centre de Bioinformatique et de Biologie Computationnelle de l'Université Laval. Part of the computations were performed on the supercomputer Colosse at Laval University, managed by Calcul Québec and Compute Canada. The operation of this supercomputer is funded by the Canada Foundation for Innovation (CFI), RMGA and the Fonds de recherche du Québec - Nature et technologies (FRQ-NT). The authors also wish to thank Dr. Dennis Nandlall from DRDC Valcartier for his fruitful discussions and his linguistic revision of the manuscript.

References

1. Abou-Rachid, H., Lussier, L.-S., Ringuette, S., Lafleur-Lambert, X., Jaidann, M., and Brisson, J., (2008) On the Correlation between Miscibility and Solubility Properties of Energetic Plasticizers/Polymer Blends: Modeling and Simulation Studies, *Propel., Explos., Pyrotech.*, **33**(4), pp. 301–310.
2. Afanas'ev, G.T. and Bobolev, V.K., (1970) *Initiation of Solid Explosives by Impact*, Springfield: Coronet Books, p. 124.
3. Agrawal, J.P., (2010) *High Energy Materials - Propellants, Explosives and Pyrotechnics*, Weinheim: Wiley-VCH, p. 495
4. Andersen, H.C., (1980) Molecular Dynamics Simulations at Constant Pressure and/or Temperature, *J. Chem. Phys.*, **72**(4), pp. 2384–2393.
5. Belik, A.V., Potemkin, V.A., and Sluka, S.N., (1999) Shock Sensitivity Analysis of Organic Explosives, *Combust. Explos. Shock.*, **35**(5), pp. 562–567.
6. Bowden, F.P. and Yoffe, A.D., (1952) *Initiation and Growth of Explosion in Liquids and Solids* Cambridge: Cambridge University Press, p. 104.
7. Brochu, D., Jaidann, M., Abou-Rachid, H., Neidert, J., and Brisson, J., (2013) Molecular Modeling: : Toward a Realistic Approach to Model Energetic Materials, *Int. J. Energetic Mat. Chem. Propuls.*, **12**(4), pp. 319–333.

8. Bunte, S.W. and Sun, H., (2000) Molecular Modeling of Energetic Materials: The Parameterization and Validation of Nitrate Esters in the COMPASS Force Field, *J. Phys. Chem. B*, **104**(11), pp. 2477–2489.
9. Chaoyang, Z., Yuanjie, S., Yigang, H., and Xinfeng, W., (2005) Theoretical Investigation of the Relationship between Impact Sensitivity and the Charges of the Nitro Group in Nitro Compounds, *J. Energ. Mater.*, **23**(2), pp. 107–119.
10. Chaudhri, M.M. and Field, J.E., (1974) The Role of Rapidly Compressed Gas Pockets in the Initiation of Condensed Explosives, *Proc. R. Soc. London A*, **340**(1620), pp. 113–128.
11. Choi, C.S. and Prince, E., (1972) The Crystal Structure of Cyclotrimethylenetrinitramine, *Acta Crystallogr., Sect. B: Struct. Sci.*, **28**(9), pp. 2857–2862.
12. Coffey, C.S., (1981) Phonon Generation and Energy Localization by Moving Edge Dislocations, *Phys. Rev. B*, **24**(12), pp. 6984–6990.
13. Coley, G.D. and Field, J.E., (1973) The Role of Cavities in the Initiation and Growth of Explosion in Liquids, *Proc. R. Soc. London A*, **335**(1600), pp. 67–86.
14. Czerski, H. and Proud, W.G., (2007) Relationship Between the Morphology of Granular Cyclotrimethylene-Trinitramine and its Shock Sensitivity, *J. Appl. Phys.*, **102**(11), pp. 113515–8.
15. Daniel, M.A., (2006), *Polyurethane Binder Systems for Polymer Bonded Explosives*, Edinburgh, AU: Australian Department of Defence, DSTO, p. 34.

16. Dixon, W.J. and Mood, A.M., (1948) A Method for Obtaining and Analyzing Sensitivity Data, *J. Am. Stat. Assoc.*, **43**(241), pp. 109–126.
17. Field, J.E., (1992) Hot Spot Ignition Mechanisms for Explosives, *Acc. Chem. Res.*, **25**(11), pp. 489–496.
18. Field, J.E., Swallowe, G.M., and Heavens, S.N., (1982) Ignition Mechanisms of Explosives during Mechanical Deformation, *Proc. R. Soc. London A*, **382**(1782), pp. 231–244.
19. Jaidann, M., Abou-Rachid, H., Lafleur-Lambert, X., Lussier, L.-S., Gagnon, N., and Brisson, J., (2008) Modeling and Measurement of Glass Transition Temperatures of Energetic and Inert Systems, *Polym. Eng. Sci.*, **48**(6), p. 10.
20. Jaidann, M., Lussier, L.-S., Bouamoul, A., Abou-Rachid, H., and Brisson, J., (2009) Effects of Interface Interactions on Mechanical Properties in RDX-Based PBXs HTPB-DOA: Molecular Dynamics Simulations. *Proc. of the 9th Intl. Conf. on Comp. Sc.*, **5545**, pp. 131–140.
21. Joseph, M.D., Jangid, S.K., Satpute, R.S., Polke, B.G., Nath, T., Asthana, S.N., and Rao, A.S., (2009) Studies on Advanced RDX/TATB Based Low Vulnerable Sheet Explosives with HTPB Binder, *Propellants, Explos., Pyrotech.*, **34**(4), pp. 326–330.
22. Jun, Z., Xin-lu, C., Bi, H., and Xiang-dong, Y., (2006) Neural Networks Study on the Correlation Between Impact Sensitivity and Molecular Structures for Nitramine Explosives, *Struct. Chem.*, **17**(5), pp. 501–507.

23. Kamlet, M.J. and Adolph, H.G., (1979) The Relationship of Impact Sensitivity with Structure of Organic High Explosives. II. Polynitroaromatic Explosives, *Propel., Explos., Pyrotech.*, **4**(2), pp. 30–34.
24. Li, M., Li, F., and Shen, R., (2011) Molecular Dynamics Simulation of Binding Energies, Mechanical Properties and Energetic Performance of the RDX/BAMO Propellant, *Acta Physico-Chemica Sinica*, **27**(6), pp. 1379–1385.
25. Li, M., Li, F., Shen, R., and Guo, X., (2011) Molecular Dynamics Study of the Structures and Properties of RDX/GAP Propellant, *J. Hazard. Mater.*, **186**(2-3), pp. 2031–2036.
26. Materials Studios 4.3, (2008) San Diego, CA, US: Accelrys Inc.
27. Matheson, R.R., (1987) Significance of Entropic Factors in Mechanical Deformation of Polymeric Glasses, *Macromol.*, **20**(8), pp. 1847–1851.
28. Mathieu, D., (2013) Toward a Physically Based Quantitative Modeling of Impact Sensitivities, *J. Phys. Chem. A*, **117**(10), pp. 2253–2259.
29. Mathieu, D. and Alaime, T., (2014) Predicting Impact Sensitivities of Nitro Compounds on the Basis of a Semi-empirical Rate Constant, *J. Phys. Chem. A*, **118**(41), pp. 9720–9726.
30. Meirovitch, H., (1983) Computer Simulation of Self-Avoiding Walks: Testing the Scanning Method, *J. Chem. Phys.*, **79**(1), pp. 502–508.

31. Metatla, N. and Soldera, A., (2011) Effect of the Molar Volume on the Elastic Properties of Vinylic Polymers: A Static Molecular Modeling Approach, *Macromol. Theory Simul.*, **20**(4), pp. 266–274.
32. Nath, T., Asthana, S.N., and Gharia, J.S., (1997) Studies on RDX Based Sheet Explosives with EVA and Estane Binders, Theory and practice of energetic material. *Proc. 2nd Int. Autumn Seminar on Propel., Explos. and Pyrotech.*, **2**, pp. 87–90.
33. Parrinello, M. and Rahman, A., (1982) Strain Fluctuations and Elastic Constants, *J. Chem. Phys.*, **76**(5), pp. 2662–2666.
34. Politzer, P. and Murray, J.S., (2003) *Theoretical and computational chemistry - Energetic Materials Part 1 Decomposition, Crystal and Molecular Properties*. Amsterdam: Elsevier, p. 465
35. Price, D. and Liddiard, T.P., (1966) *The Small Scale Gap Test Calibration and comparison with the Large Scale Gap Test.*, White Oak, US: United States Naval Ordnance Laboratory, p. 59.
36. Qiu, L., Zhu, W.-H., Xiao, J.-J., Zhu, W., Xiao, H.-M., Huang, H., and Li, J.-S., (2007) Molecular Dynamics Simulations of trans-1,4,5,8-Tetranitro-1,4,5,8-tetraazadecalin-Based Polymer-Bonded Explosives, *J. Phys. Chem. B*, **111**(7), pp. 1559–1566.
37. Rice, B.M. and Hare, J.J., (2002) A Quantum Mechanical Investigation of the Relation between Impact Sensitivity and the Charge Distribution in Energetic Molecules, *J. Phys. Chem. A*, **106**(9), pp. 1770–1783.

38. Rideal, E.K. and Robertson, A.J.B., (1948) The Sensitiveness of Solid High Explosives to Impact, *Proc. R. Soc. London A*, **195**(1041), pp. 135–150.
39. Sartomer Company Inc., (2011) *Hydroxyl Terminated Polybutadiene Resins and Derivatives Product Bulletin*, Sartomer Company, Inc., Exton, PA.
40. Small Arm Survey, (2012) *Unplanned Explosions at Munitions Sites*, accessed Dec. 12, 2012, from <http://www.smallarmssurvey.org/?uems>.
41. Soldera, A., (2002) Energetic Analysis of the two PMMA Chain Tacticities and PMA Through Molecular Dynamics Simulations, *Polymer*, **43**(15), pp. 4269–4275.
42. Soldera, A., (2012) Atomistic Simulations of Vinyl Polymers, *Mol. Simul.*, **38**(8-9), pp. 762–771.
43. Sun, H., (1998) COMPASS: An ab Initio Force-Field Optimized for Condensed-Phase Applications Overview with Details on Alkane and Benzene Compounds, *J. Phys. Chem. B*, **102**(38), pp. 7338–7364.
44. Theodorou, D.N. and Suter, U.W., (1986) Atomistic Modeling of Mechanical Properties of Polymeric Glasses, *Macromol.*, **19**(1), pp. 139–154.
45. van der Heijden, A.E.D.M. and Bouma, R.H.B., (2004), Crystallization and Characterization of RDX, HMX, and CL-20, *Cryst. Growth Des.*, **4**(5), pp. 999–1007.
46. Xiao, J., Huang, H., Li, J., Zhang, H., Zhu, W., and Xiao, H., (2008), Computation of Interface Interactions and Mechanical Properties of HMX-based PBX with Estane 5703 from Atomic Simulation, *J. Mater. Sci.*, **43**(17), pp. 5685–5691.

47. Xu, X.-J., Xiao, H.-M., Xiao, J.-J., Zhu, W., Huang, H., and Li, J.-S., (2006) Molecular Dynamics Simulations for Pure ϵ -CL-20 and ϵ -CL-20-Based PBXs, *J. Phys. Chem. B*, **110**(14), pp. 7203–7207.
48. Xu, X., Xiao, J., Huang, H., Li, J., and Xiao, H., (2007) Molecular dynamics simulations on the structures and properties of ϵ -CL-20-based PBXs, *Sci. China, Ser. B: Chem.*, **50**(6), pp. 737–745.
49. Yadav, H.S., Nath, T., Sundaram, S.G., Kamath, P.V., and Kulkarni, M.W., (1994) Shock Initiation of Sheet Explosive, *Propellants, Explos., Pyrotech.*, **19**(1), pp. 26–31.
50. Yang, J., Ren, Y., Tian, A.-M., and Sun, H., (2000) COMPASS Force Field for 14 Inorganic Molecules, He, Ne, Ar, Kr, Xe, H₂, O₂, N₂, NO, CO, CO₂, NO₂, CS₂, and SO₂, in Liquid Phases, *J. Phys. Chem. B*, **104**(20), pp. 4951–4957.
51. Zhu, W., Xiao, J., Zhu, W., and Xiao, H., (2009) Molecular Dynamics Simulations of RDX and RDX-based Plastic-Bonded Explosives, *J. Hazard. Mater.*, **164**(2-3), pp. 1082–1088.

Figure 1 – Energetic molecule (RDX), polymers (HTPB, Estane and EVA) and plasticizer

(DOA) simulated in this work

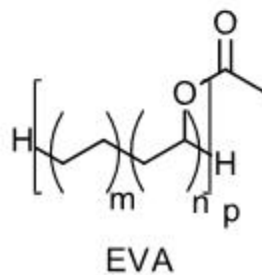
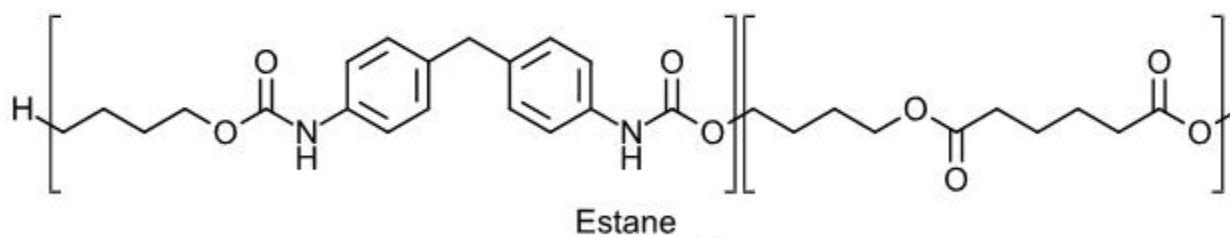
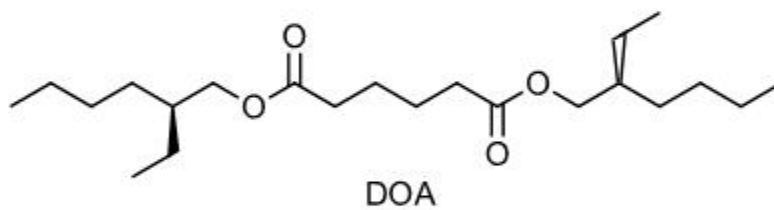
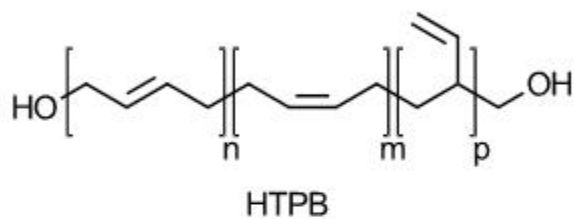
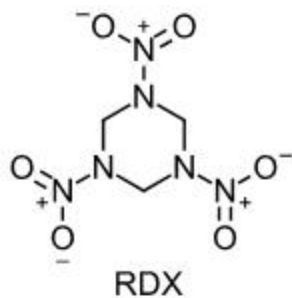


Figure 2 – Construction of a PBX supercell

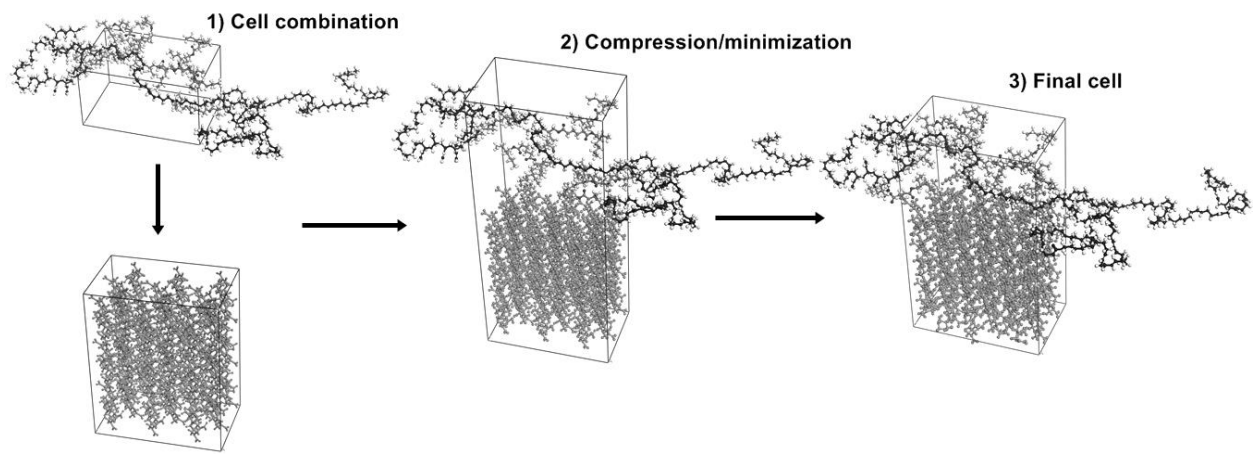


Figure 3 – Density adjustment of the supercell by compression/minimization steps

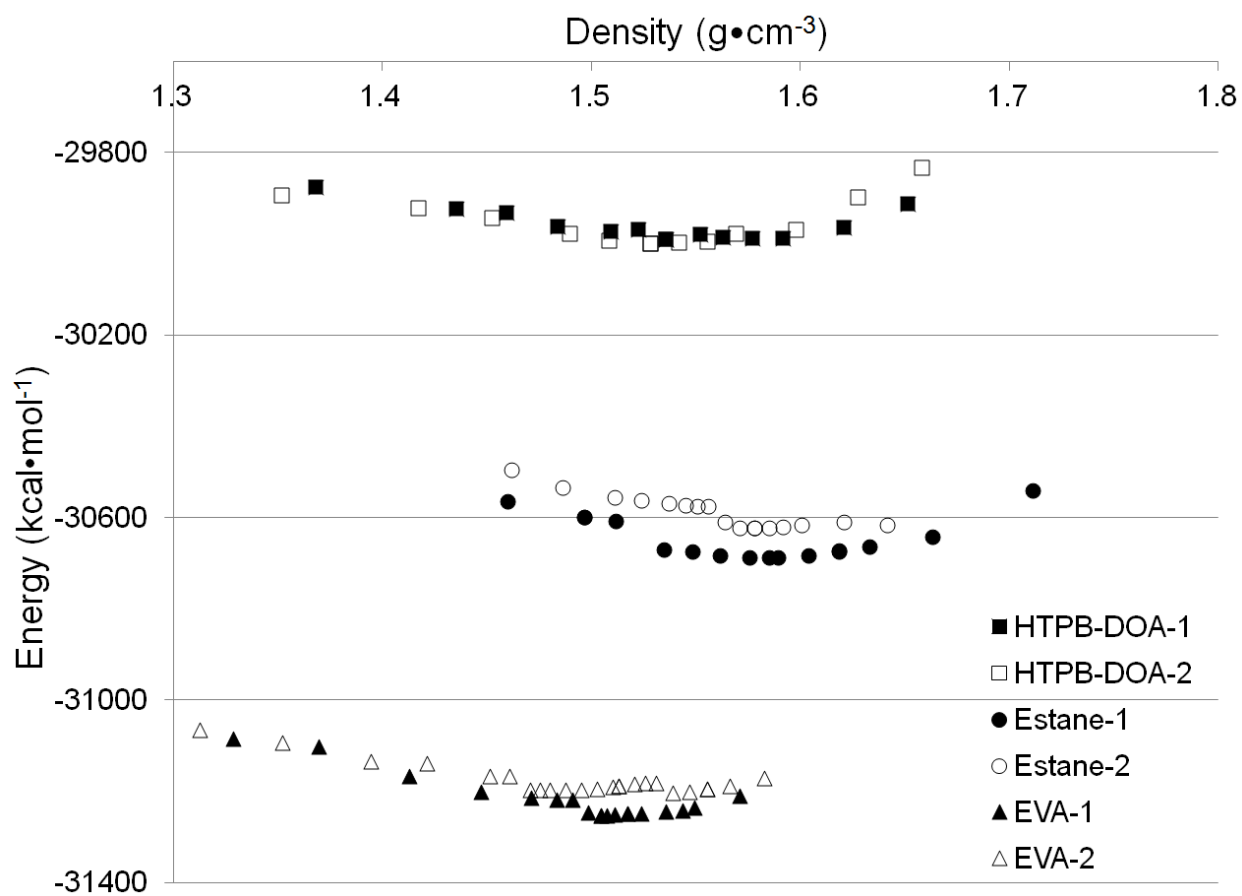


Figure 4 – Typical examples of a polymer cell (right), a crystalline explosive cell (middle) and a cell of the complete formulation (left)

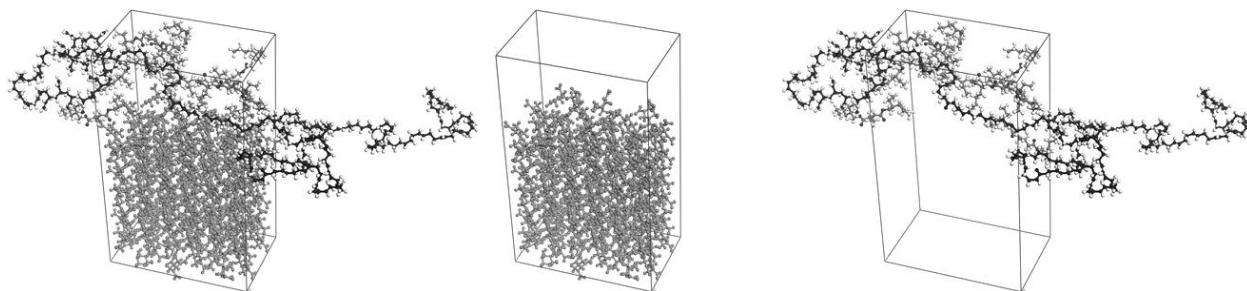


Figure 5 - Energy increases (kcal/mol) of the explosive and polymer for the various PBX models simulated

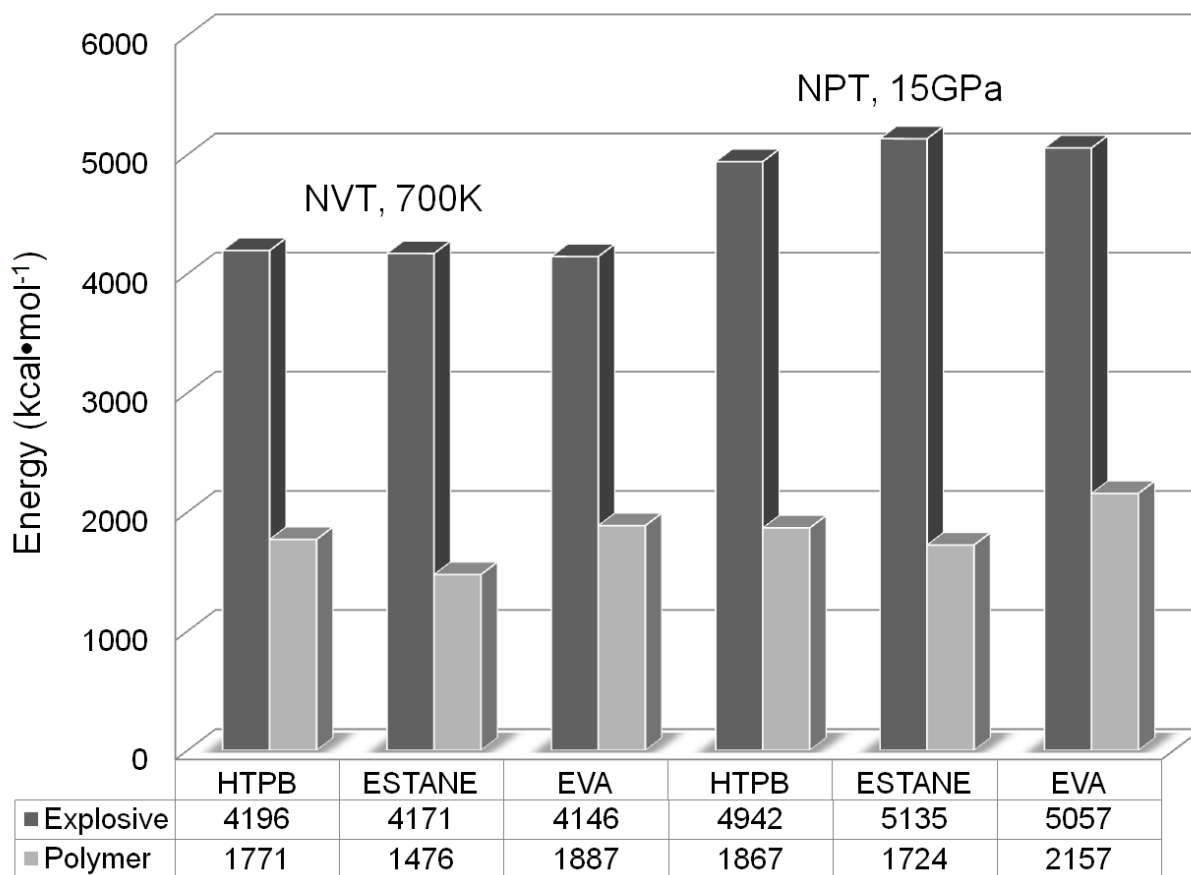
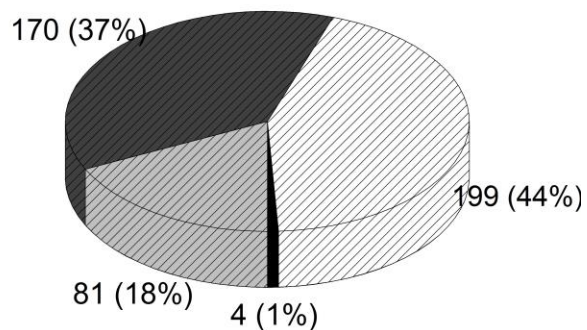
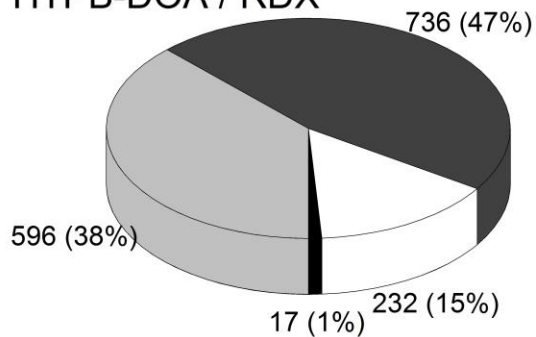
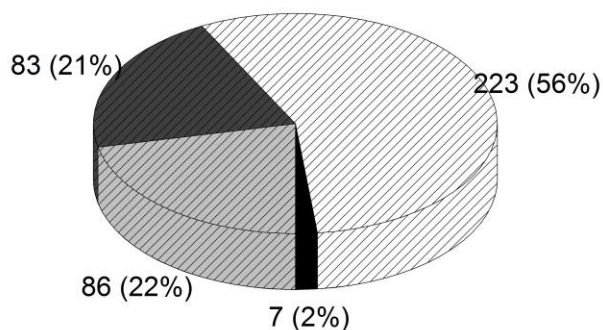
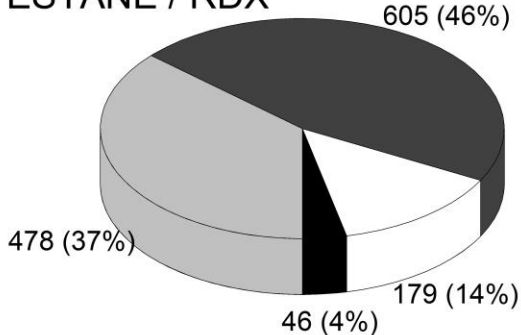


Figure 6 – Detailed contributions to internal energy of the polymer

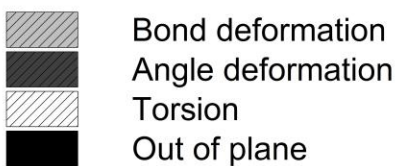
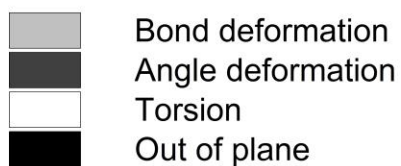
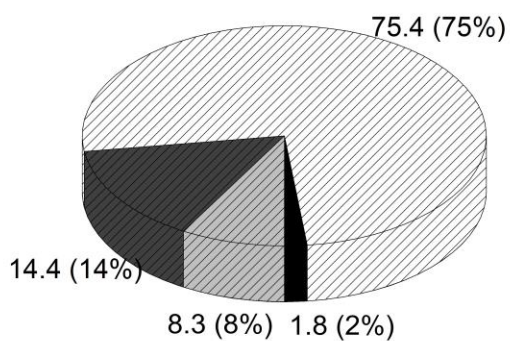
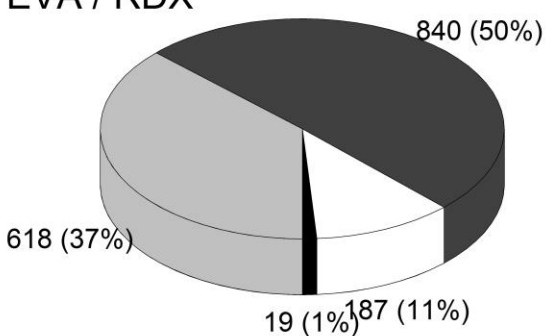
HTPB-DOA / RDX



ESTANE / RDX



EVA / RDX



DOCUMENT CONTROL DATA

*Security markings for the title, authors, abstract and keywords must be entered when the document is sensitive

1. ORIGINATOR (Name and address of the organization preparing the document. A DRDC Centre sponsoring a contractor's report, or tasking agency, is entered in Section 8.) International Journal of Energetic Materials and Chemical Propulsion		2a. SECURITY MARKING (Overall security marking of the document including special supplemental markings if applicable.) CAN UNCLASSIFIED
		2b. CONTROLLED GOODS NON-CONTROLLED GOODS DMC A
3. TITLE (The document title and sub-title as indicated on the title page.) Sensitivity of polymer-bonded explosives from molecular modeling data		
4. AUTHORS (Last name, followed by initials – ranks, titles, etc., not to be used) Brochu, D., Abou-Rachid, H.; Soldera, A.; Brisson, J.		
5. DATE OF PUBLICATION (Month and year of publication of document.) July 2018	6a. NO. OF PAGES (Total pages, including Annexes, excluding DCD, covering and verso pages.) 0	6b. NO. OF REFS (Total references cited.) 0
7. DOCUMENT CATEGORY (e.g., Scientific Report, Contract Report, Scientific Letter.) External Literature (P)		
8. SPONSORING CENTRE (The name and address of the department project office or laboratory sponsoring the research and development.) DRDC - Valcartier Research Centre Defence Research and Development Canada 2459 route de la Bravoure Quebec (Quebec) G3J 1X5 Canada		
9a. PROJECT OR GRANT NO. (If appropriate, the applicable research and development project or grant number under which the document was written. Please specify whether project or grant.)	9b. CONTRACT NO. (If appropriate, the applicable number under which the document was written.)	
10a. DRDC PUBLICATION NUMBER (The official document number by which the document is identified by the originating activity. This number must be unique to this document.) DRDC-RDDC-2018-P091	10b. OTHER DOCUMENT NO(s). (Any other numbers which may be assigned this document either by the originator or by the sponsor.)	
11a. FUTURE DISTRIBUTION WITHIN CANADA (Approval for further dissemination of the document. Security classification must also be considered.) Public release		
11b. FUTURE DISTRIBUTION OUTSIDE CANADA (Approval for further dissemination of the document. Security classification must also be considered.)		

12. KEYWORDS, DESCRIPTORS or IDENTIFIERS (Use semi-colon as a delimiter.)

PBX; Energetic materials; Molecular modeling; RDX; HTPB; Computational chemistry

13. ABSTRACT/RÉSUMÉ (When available in the document, the French version of the abstract must be included here.)